Prolonged myelination in human neocortical evolution

Daniel J. Miller[a], Tetyana Duka[a], Cheryl D. Stimpson[a], Steven J. Schapiro[b], Wallace B. Baze[b], Mark J. McArthur[b], Archibald J. Fobbs[c], André M. M. Sousa[d,e], Nenad Šestan[d], Derek E. Wildman[f], Leonard Lipovich[f], Christopher W. Kuzawa[g], Patrick R. Hof[h,i], and Chet C. Sherwood[a,1]

[a]Department of Anthropology, The George Washington University, Washington, DC 20052; [b]Department of Veterinary Sciences, University of Texas M. D. Anderson Cancer Center, Bastrop, TX 78602; [c]National Museum of Health and Medicine, SIlver Spring, MD 20910; [d]Department of Neurobiology and Kavli Institute for Neuroscience, Yale University School of Medicine, New Haven, CT 06510; [e]Graduate Program in Areas of Basic and Applied Biology, Abel Salazar Biomedical Sciences Institute, University of Porto, Porto 4099-002, Portugal;[f]Center for Molecular Medicine and Genetics, Wayne State University School of Medicine, Detroit, MI 48201; [g]Department of Anthropology, Northwestern University, Evanston, IL 60208; [h]Fishberg Department of Neuroscience and Friedman Brain Institute, Mount Sinai School of Medicine, New York, NY 10029; and [i]New York Consortium in Evolutionary Primatology, New York, NY

Edited by Fred H. Gage, The Salk Institute for Biological Studies, San Diego, CA, and approved August 14, 2012 (received for review October 31, 2011)

Nerve myelination facilitates saltatory action potential conduction and exhibits spatiotemporal variation during development associated with the acquisition of behavioral and cognitive maturity. Although human cognitive development is unique, it is not known whether the ontogenetic progression of myelination in the human neocortex is evolutionarily exceptional. In this study, we quantified myelinated axon fiber length density and the expression of myelin-related proteins throughout postnatal life in the somatosensory (areas 3b/3a/1/2), motor (area 4), frontopolar (prefrontal area 10), and visual (areas 17/18) neocortex of chimpanzees ($N = 20$) and humans ($N = 33$). Our examination revealed that neocortical myelination is developmentally protracted in humans compared with chimpanzees. In chimpanzees, the density of myelinated axons increased steadily until adult-like levels were achieved at approximately the time of sexual maturity. In contrast, humans displayed slower myelination during childhood, characterized by a delayed period of maturation that extended beyond late adolescence. This comparative research contributes evidence crucial to understanding the evolution of human cognition and behavior, which arises from the unfolding of nervous system development within the context of an enriched cultural environment. Perturbations of normal developmental processes and the decreased expression of myelin-related molecules have been related to psychiatric disorders such as schizophrenia. Thus, these species differences suggest that the human-specific shift in the timing of cortical maturation during adolescence may have implications for vulnerability to certain psychiatric disorders.

primate | hominids | neuropsychiatric illness | cortical development | behavioral maturation

Comparative studies suggest that human neurobiological development is unique. For example, humans differ from other primates in extending a rapid, fetal-like brain mass growth rate into the first postnatal year, thereby achieving relatively large adult brain size (1). Gene expression patterns related to postnatal development of the prefrontal cortex are delayed in humans compared with chimpanzees and macaque monkeys (2). In addition, synapse maturation (3, 4) and axon myelination (5, 6) occur during later life history stages in humans compared with macaques. Furthermore, recent volumetric data obtained by using in vivo MRI demonstrates that human neural development and aging differ from those of our close nonhuman primate relatives (7–9). Together, these observations indicate that a marked delay in the developmental schedule of human neocortex may play an important role in the growth of connections that contribute to our species-specific cognitive abilities by providing greater opportunities for social learning to influence the establishment of circuits.

The myelin lipid bilayer surrounding neuronal axons is crucial to normal brain function in vertebrates. Myelination results from the dynamic integration of neuron–oligodendrocyte signaling to promote saltatory action potential conduction (10). Specifically, myelination increases in response to electrical excitation and activity-dependent molecular cascades, protecting the axon from damage and significantly increasing nerve impulse transmission speed (6, 11). Myelination is important in establishing connectivity in the growing brain by facilitating rapid and synchronized information transfer across neural systems, which is essential to higher-order cognitive functions (6). Despite this crucial role, only limited data exist comparing the development of myelination in humans with our closest living relatives, chimpanzees (8).

Neocortical myelin development is disrupted in certain neuropsychiatric disorders that profoundly affect cognition in humans. Studies of patients with schizophrenia consistently indicate abnormalities in cortical white matter tracts (12–14) and decreased myelin-related mRNA and protein expression (15–18), particularly during adolescence (19). For example, expression of 2′,3′-cyclic nucleotide 3′-phosphodiesterase (CNP) and myelin-associated glycoprotein (MAG) is dysregulated in patients with schizophrenia (20–22). CNP is crucial during the initial stage of myelin growth as oligodendrocytes extend processes toward axons (23). MAG regulates later stages of neuron–oligodendrocyte interactions, providing trophic support to established axons while inhibiting neurite outgrowth (24).

A comparison of the timing of the maturation of myelin in the cerebral cortex between humans and nonhuman primates may provide insight into the evolution of human cognitive development and our vulnerability to psychiatric disorders. To clarify whether myelin growth differs in the neocortex of humans and chimpanzees, we investigated the development of myelinated fiber length density (MFLD) in the primary somatosensory area (area 3b), primary motor area (area 4), most rostral part of the prefrontal cortex (the frontopolar region, area 10), and prestriate visual cortex (area 18/V2) from histological preparations. We also analyzed developmental changes in myelin-related protein expression (i.e., CNP and MAG) in somatosensory areas (areas 3b/3a/1/2), motor area (area 4), frontopolar area (area 10), and visual cortex (areas 17/V1 and 18/V2). Aside from studies of brain size growth (1), to our knowledge, this analysis represents the largest sample of chimpanzee neural development investigated to date.

Results

All cortical regions in human and chimpanzee samples (Table S1) showed increasing myelination with age (Figs. 1 and 2). In adulthood, somatosensory, motor, frontopolar, and visual areas

Author contributions: D.J.M., T.D., S.J.S., W.B.B., M.J.M., A.J.F., D.E.W., L.L., C.W.K., P.R.H., and C.C.S. designed research; D.J.M., T.D., and C.D.S. performed research; S.J.S., W.B.B., M.J.M., A.J.F., A.M.M.S., N.S., D.E.W., L.L., and P.R.H. contributed new reagents/analytic tools; D.J.M., T.D., and C.C.S. analyzed data; and D.J.M., C.W.K., P.R.H., and C.C.S. wrote the paper.

The authors declare no conflict of interest.

This article is a PNAS Direct Submission.

[1]To whom correspondence should be addressed. E-mail: sherwood@gwu.edu.

This article contains supporting information online at www.pnas.org/lookup/suppl/doi:10.1073/pnas.1117943109/-/DCSupplemental.

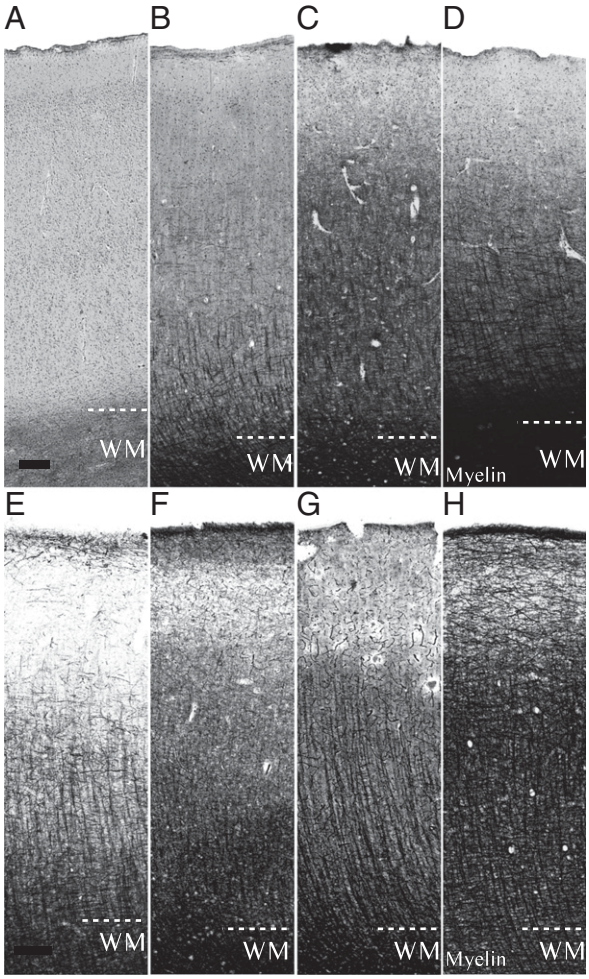

Fig. 1. Developmental series of low-magnification photos of human and chimpanzee primary motor cortex. Sections from motor cortex (area 4) stained for myelinated axons (myelin) arranged by life-history stage. (*A–D*) Representative sections of human neocortical myelin as an *A*: infant (0–1 y), (*B*) child/juvenile (3–9 y), (*C*) adolescent/young adult (13–23 y), and (*D*) adult (≥28 y). (*E–H*) Sections of chimpanzee neocortical myelin as an *E*: infant (0–2 y), (*F*) juvenile (5–6 y), (*G*) adolescent (9–11 y), and (*H*) adult (≥17 y). White matter (WM) is demarcated at the bottom of the cortex. (Scale bar: 200 μm.)

displayed regional differences in myelination that were qualitatively similar in both species (Fig. S1).

We used stereology to quantify MFLD within the gray matter of several cortical regions. MFLD in the cerebral cortex at birth in humans was extremely low (~0.008 μm/μm^3), but increased rapidly during infancy. After infancy, the rate of myelination slowed during childhood and adolescence, but exhibited continued growth until the end of the third decade. Specifically, mean MFLD during later adulthood (defined as ≥28 y) was significantly greater than in adolescence and early adulthood (11–23 y; Welch *t*, $P = 0.000059$; Mann–Whitney *U*, $P = 0.00016$). Accordingly, the developmental trajectory of cortical MFLD in the human sample was best fit by a cubic regression function for all regions (Fig. 3*A* and Table 1). Throughout life, human frontopolar cortex exhibited the lowest MFLD and the motor cortex had the highest average MFLD values.

In contrast to humans, MFLD in chimpanzees displayed a consistent rate of increase until the time of puberty, at which time fibers became maximally dense. Thus, MFLD in adult chimpanzees (≥17 y) was not significantly different from juveniles (5–11 y; Welch *t*, $P > 0.785$; Mann–Whitney *U*, $P > 0.848$). Furthermore, the developmental trajectory of MFLD in the chimpanzee sample was best fit by a linear model for frontopolar cortex, and by quadratic regression functions for the other regions (Fig. 3*B* and Table 1). Overall, like humans, the frontopolar cortex exhibited the lowest MFLD and motor cortex had the highest average MFLD values throughout development.

To represent the relative degree of MFLD maturation at different developmental stages in each species, we calculated the percentage of values from the adult mean. Whereas human infants have less than 2% of maximal adult-like MFLD and achieve only ~60% during adolescence, chimpanzee infants have ~20% and attain nearly 96% maximal MFLD during adolescence (Fig. 3*C* and Table S2).

To examine whether the observed differences between humans and chimpanzees in the developmental progression of MFLD is related to species differences in the expression of proteins that are important in regulating myelination, we performed Western blot analyses of MAG and CNP. Overall, MAG and CNP protein expression tended to increase with age in both species, although some cortical regions did not exhibit a significant association with age in our samples (Fig. 4, Figs. S2 and S3, and Table S3). Notably, the age-related effects for MAG and CNP protein expression were gradual linear or quadratic increases, which differ from the distinctive pattern of extended childhood and continued post-adolescent myelin growth observed in humans for MFLD.

Discussion

Our data demonstrate that the developmental trajectory of neocortical myelination in humans is distinct compared with chimpanzees. Humans are born with fewer myelinated axons compared with chimpanzees, and prolong myelin growth well beyond adolescence. By using stereologic methods to analyze the length density of myelinated axon fibers within the gray matter of the cerebral cortex, we also corroborated previous observations based on histological and neuroimaging techniques, indicating that myelin develops in primary cortical areas before association cortical areas (5–7, 25–28). The infant, juvenile, and adolescent stages are periods of intense learning in primates. The convergence of neural

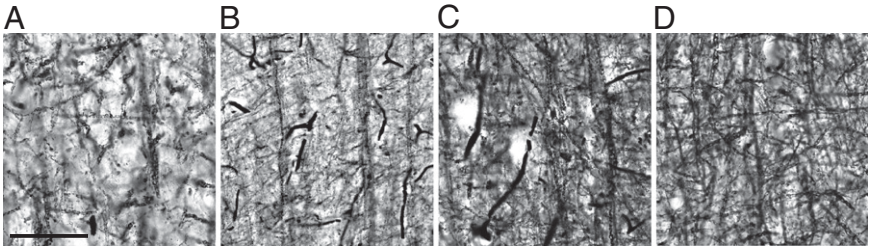

Fig. 2. Developmental series of high-magnification photomicrographs of layer III in chimpanzee primary motor cortex. Representative photomicrographs of layer III of primary motor cortex (area 4) in chimpanzee tissue sections stained for myelin using the Gallyas preparation. Images are arranged by life-history stage: (*A*) infant (0–2 y), (*B*) juvenile (5–6 y), (*C*) adolescent (9–11 y), and (*D*) adult (≥17 y). (Scale bar: 50 μm.)

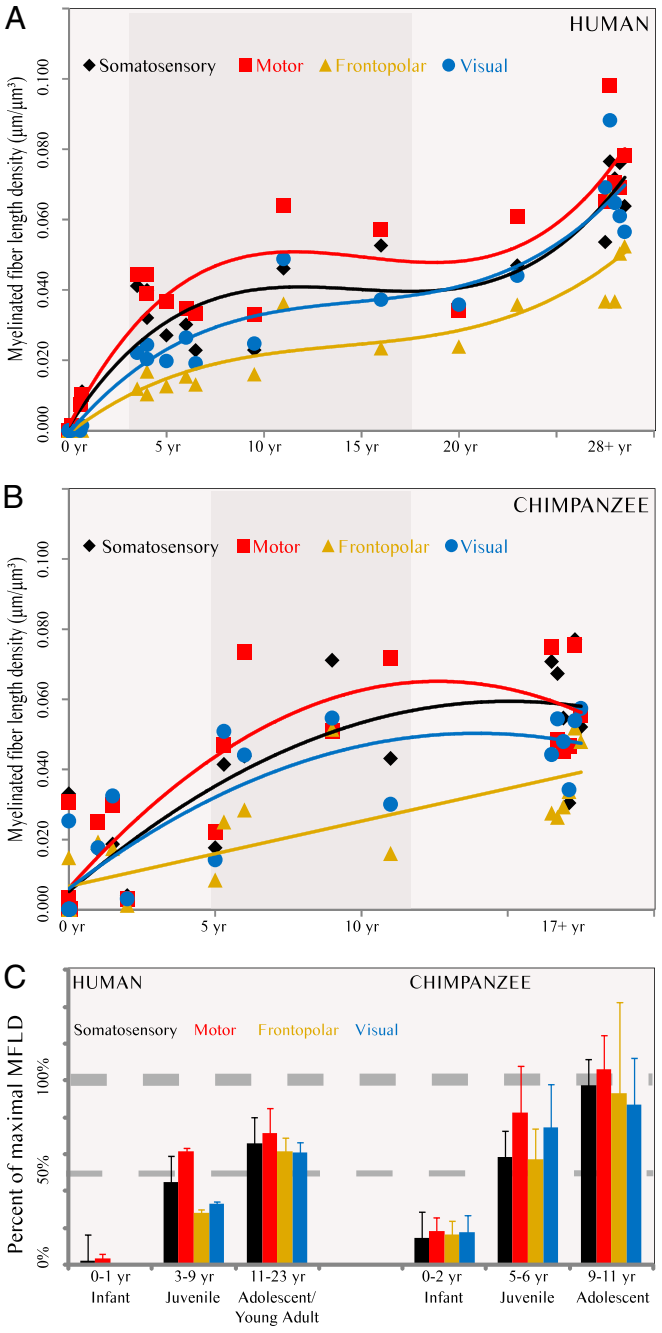

Fig. 3. Developmental trajectory of MFLD. Graphs show best-fit curves for MFLD data in humans (*A*; $n = 24$) and chimpanzees (*B*; $n = 20$) arranged by age in years. The shaded vertical area represents time between weaning and full sexual maturation. Diamonds represent somatosensory area (area 3b), squares represent motor area (area 4), triangles represent frontopolar area (area 10), and circles represent visual area (area 18). (*C*) Bar graph depicts mean percent of maximum mature adult MFLD across development in humans (*Left*) and chimpanzees (*Right*). Error bars represent SEM. The thin and thick horizontal dashed lines represent 50% and 100%, respectively, of maximum MFLD. Black represents somatosensory area (area 3b), red represents motor area (area 4), gold represents frontopolar area (area 10), and blue represents visual area (area 18).

growth with social and environmental factors during these periods mediates cognition in crucial ways, particularly given the extended lifespan and enriched cultural context of humans (29). Therefore, evolutionary modification of the developmental schedule of neural connectivity in humans might contribute to the formation

Table 1. Best-fit regression functions for myelinated fiber density data

Function	Function	Adjusted R^2	*P* value
Human			
Somatosensory	Cubic	0.883	0.002
Motor	Cubic	0.884	0.001
Frontopolar	Cubic	0.878	0.034
Visual	Cubic	0.924	0.001
Chimpanzee			
Somatosensory	Quadratic	0.733	0.061
Motor	Quadratic	0.722	0.006
Frontopolar	Linear	0.573	0.001
Visual	Quadratic	0.687	0.032

Values calculated by using hierarchical multiple regression analysis with adults as endpoint (*Materials and Methods*).

of functional circuitry with greater plasticity, simultaneously contributing to unique species-specific pathological vulnerability to schizophrenia and other psychiatric disorders.

Myelination is ubiquitous throughout the nervous system of vertebrates and plays a dynamic role in regulating the functional activity of axons (10, 11). The myelin sheath is therefore crucial to normal neurological function, and the density of myelinated axons is commonly used to assess the relative maturity of brain regions. Traditionally, histological studies of myelin growth have been qualitative, making direct ontogenetic comparisons between species difficult (5, 6, 30–37). Nonetheless, previous studies (5, 6) described greater initial myelination of the cerebral cortex in neonatal macaque monkeys compared with humans. Our data provide further evidence that the lack of myelination in the newborn human neocortex is distinct from our closest living phylogenetic relatives, indicating that a greater fraction of mature adult-like neocortical myelination is achieved before birth in chimpanzees (~20%) compared with humans (~0%). The relative absence of myelin in the neonatal human cortex complements other data showing that, at the time of birth, human brains are a relatively small proportion of their adult size (27%) compared with chimpanzees (36%) (38), and that much of postnatal brain expansion results from the growth of white matter underlying the neocortex (8, 25). Together, these observations suggest that activity-mediated myelin growth early in human life has the capacity to be shaped by postnatal environmental and social interactions to a greater degree than in other primates, including chimpanzees.

Later myelin growth also differentiates humans and chimpanzees. Our data demonstrate that, in chimpanzees, the density of myelinated axons reaches its maximum level by adolescence for most cortical regions. Notably, we found a gradual linear trend of increasing MFLD beyond adolescence in frontopolar cortex. This is similar to results from histological and neuroimaging studies of macaque monkeys indicating that the growth of cortical myelination and the volume of the underlying white matter are largely complete by puberty (5, 7, 8). In contrast, we found that pronounced increases in the density of myelinated axons in the human neocortex continue after adolescence and into the third decade, providing further evidence of extraordinary prolonged neocortical maturation. MRI studies also indicate that growth in the volume of the cortical white matter persists well beyond puberty (25–28, 39). Additionally, in humans, neocortical dendritic development and synaptogenesis exhibit heterogeneity across the processing hierarchy, with the greatest delay in maturation characterizing the prefrontal cortex (40–44). Synaptic pruning in human prefrontal cortex has been shown to continue until age 30 y (4). These neuroanatomical findings are congruent with recent evidence indicating widespread delay in the gene expression profile of the human prefrontal cortex compared with chimpanzees and macaque

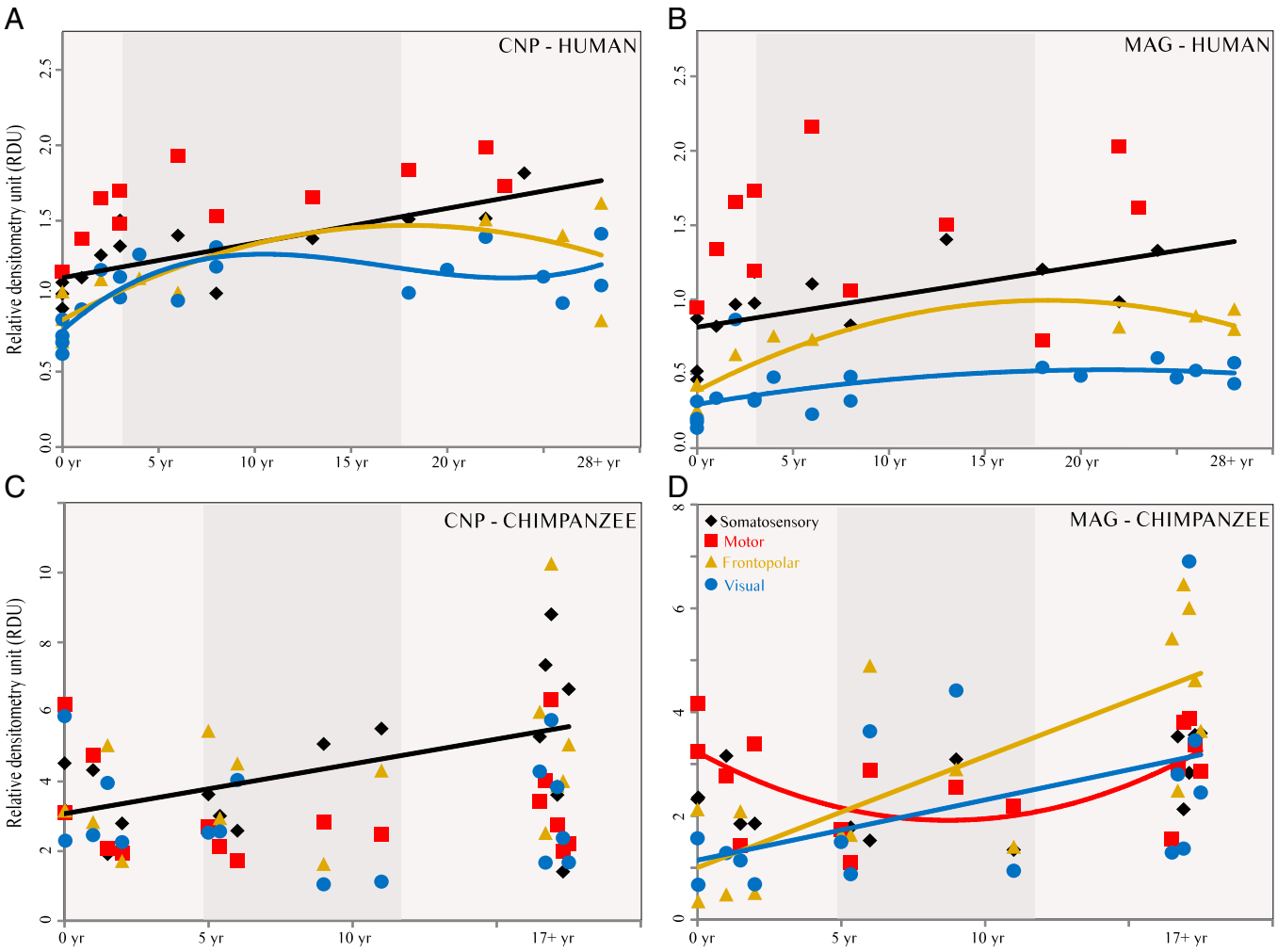

Fig. 4. Developmental trajectory of MAG and CNP protein. Graphs depict best-fit curves for densitometric analyses in relative densitometry units of CNP (*A* and *C*) and MAG (*B* and *D*) protein expression in humans (*A* and *B*; $n = 23$) and chimpanzees (*C* and *D*: $n = 16$) arranged by age in years. The shaded vertical area represents time between weaning and full sexual maturation. Trend lines represent a significant effect of age at the $P \leq 0.05$ level. Diamonds represent somatosensory area (area 3b/3a/1/2), squares represent motor area (area 4), triangles represent frontopolar area (area 10), and circles represent visual area (areas 17 and 18). Note the different scales for relative densitometry units between species because Western blotting was performed on frozen human cortical samples, whereas, in chimpanzees, samples were formalin-fixed.

monkeys (2). In sum, these species differences suggest that neural development in humans is characterized by a number of features that prolong the process of neocortical maturation.

Given that humans and chimpanzees displayed divergent growth trends for myelinated axon density in the neocortex, we sought to explore the potential molecular mechanisms regulating these species differences by analyzing the expression of CNP and MAG, two proteins that contribute to distinct aspects of myelin development. CNP protein facilitates oligodendrocyte differentiation and process outgrowth early in the myelination process (45, 46), whereas MAG is important in oligodendrocyte–neuron signaling, such that it regulates axon caliber and contributes to axon growth cone collapse, maintaining established axons at the expense of novel growth (24, 47, 48). The results from Western blotting for CNP and MAG, however, did not reveal developmental changes in myelin-associated protein expression in humans that mirrored the cubic function of the MFLD curve. Indeed, the postnatal developmental regulation of CNP and MAG was modest compared with the more dramatic anatomical changes in MFLD in both species. The molecular mechanisms responsible for the evolution of prolonged myelination of the cerebral cortex in humans remain incompletely understood, and further research with other myelin-related genes, more sensitive techniques, and larger samples is needed.

The evolutionary significance of prolonged myelination in humans is uncertain. One possibility is that additional postpubertal growth of myelination is a byproduct of alterations to earlier life history stages in human evolution, such as an extended period of slow childhood growth (49). An alternative hypothesis is that there has been selection on changes to the neural circuitry mediating learning and memory following the time of sexual maturity. There are well-documented changes to executive and social cognitive functions that characterize adolescence in humans, presumably related to the growth of myelination and white matter tracts, including improvements in selective attention, decision-making, inhibitory control, working memory, and perspective-taking (50). Unfortunately, comparable data are not available to determine whether chimpanzees or other primates undergo such dramatic transformations of cognitive abilities after puberty.

Sustained postpubertal myelin growth, which is unique to humans, might be associated with our species-specific vulnerability to certain psychiatric diseases that display onset during adolescence and early adulthood. Previous research has identified abnormal myelination in a number of psychiatric diseases that may derive

from the disruption of normal postnatal development (51). For example, schizophrenia is associated with abnormal myelination of the cortical white matter, particularly in the prefrontal cortex (52). Molecular studies also implicate disrupted myelin-related processes throughout the forebrain, such as CNP and MAG gene or protein expression, in the pathogenesis of schizophrenia (14–22).

Accumulating evidence suggests that adolescence and young adulthood constitute a novel period in the evolution of human neurobiological development (1–4, 7, 28, 49, 53). Our findings extend this observation to the ontogeny of myelination, which follows a distinctively delayed and prolonged pattern of development in humans. These results invite further exploration of the molecular and systems-level mechanisms that mediate plasticity and learning that are unique to the human species, as these are not only important for normal cognition and adaptive behavior, but may also be crucial in the emergence of certain psychiatric disorders.

Materials and Methods

Sample and Preparation. The study sample consisted of postmortem brains from a total of 33 humans (*Homo sapiens,* 16 male and 17 female) and 20 common chimpanzees (*Pan troglodytes*, 13 male and 7 female), ranging in age from birth to adulthood (Table S1). The human histological sample was drawn from the Yakovlev–Haleem slide collection (n = 24) at the National Museum of Health and Medicine. These sections were cut at 35 μm and stained for myelin with the Loyez method (6). Additional human samples were used for Western blotting and for examination of the effect of different myelin staining techniques on the results. These additional frozen and fixed human cortical tissue samples were obtained from the National Institute of Child Health and Human Development Brain and Tissue Bank for Developmental Disorders at the University of Maryland (Baltimore, MD; n = 9). Other frozen human samples that were used for Western blotting were obtained from the laboratory of Nenad Šestan (Yale University School of Medicine, New Haven, CT; full details provided in ref. 54). All human brain specimens originated from individuals free of neurological or psychiatric disorders. The same chimpanzee sample was used for histology and Western blotting, and it included formalin-fixed brains or dissected blocks collected from various research institutions (*SI Materials and Methods* and Table S1). The chimpanzee cortical samples were sectioned at 40 μm, every 10th section was stained for Nissl substance to reveal cytoarchitecture, and an adjacent 1-in-10 series was stained to visualize myelin using the Gallyas method (55). No neurological deficits were detected in any of the chimpanzees included in this study, and all brains appeared normal on routine inspection at necropsy. All histological sections from humans and chimpanzees appeared free of neuropathologic processes. Tissue samples were randomly coded to prevent observer bias in stereologic quantification and Western blotting; however, this was not feasible for the Yakovlev–Haleem slide collection. We did not examine sex differences because of limited tissue availability.

Stereology. All quantification of MFLD was performed by the same observer (D.J.M.) by using Stereo Investigator software (MBF Bioscience). MFLD was calculated from sections stained for myelin at high magnification (≥60×; *SI Materials and Methods*) using a 6-μm SpaceBalls probe under Koehler illumination (56) in ∼90 sampling locations per region in each individual (17,550 total sampling locations; 9,450 in humans and 8,100 in chimpanzees). Curved portions of the cortical mantle were avoided when defining regions of interest for length density measurement.

Reliability of Results Between Different Myelin Staining Methods. Because the stereologic quantification of MFLD in humans used sections stained for myelin with the Loyez method and the chimpanzee sections were stained with the Gallyas method, we sought to determine the reliability of results across these techniques. We compared MFLD between the different myelin stains in chimpanzee cortical sections from two regions (motor and frontopolar cortex) and in individuals of five different ages and found a high degree of correlation (Pearson adjusted R^2 = 0.576, P = 0.007; Spearman adjusted R^2 = 0.521, P = 0.011; n = 10; Fig. S4). Additionally, sections from human frontopolar cortex stained by using the Gallyas technique showed a significant cubic trajectory for MFLD, similar to that observed with the Loyez stain (adjusted R^2 = 0.006, n = 9; Fig. S5). Chimpanzee sections stained using the Loyez technique show similar results for age-related changes in MFLD to those obtained with the Gallyas stain. Motor cortex was best fit by a quadratic model (adjusted R^2 = 0.921, P = 0.006; n = 5; Fig. S6) and frontopolar cortex by a linear regression function (adjusted R^2 = 0.921, P = 0.006; n = 5; Fig. S6).

Western Blot Analyses. Western blotting was performed as described previously (57) with minor modifications. Fig. S3 shows results for Western blot validation using polyclonal anti-MAG (1:300; LifeSpan BioSciences) and monoclonal anti-CNP antibodies (1:300; Abcam). GAPDH (Imgenex) and β-actin (1:1,000; Santa Cruz Biotechnology) were used as loading controls to normalize expression levels. Densitometry analyses of Western blots were performed using Scion Image software (Fig. S3*C*). Full details of the Western blot assay are provided in *SI Materials and Methods*.

Statistical Methods. The SPSS package was used for statistical analyses. For the calculation of best-fit regression curves depicting growth effects in MFLD and protein expression during development, we grouped older adult values together to summarize variability in each species because our aim was to focus on the trajectory of earlier developmental changes. Regression curves were calculated by using forward-selection multiple regression for linear, quadratic, and cubic functions (58). Age groups were determined based on life history stages (38, 49, 53), punctuated by the species-typical age at weaning (human, ∼3 y; chimpanzee, ∼5 y) and puberty (human, ∼11–14 y; chimpanzee, ∼8–10 y) (59, 60). Adult age was assigned as the age of the youngest postpubertal individual in the sample, except in humans in whom MFLD showed a significant difference between older (≥28 y) and younger (<28 y) adults (*Results*); mature adult age was thus assigned at 28 y. P values lower than 0.05 were considered significant.

ACKNOWLEDGMENTS. The authors thank Drs. William Hopkins and Joseph Erwin for facilitating access to brain specimens; and Drs. Robin Bernstein, Shannon McFarlin, and James Steiger for helpful discussion related to this research. This work was supported by National Science Foundation Grants BCS-0515484, BCS-0549117, BCS-0824531, and DGE-0801634; National Institutes of Health Grants NS-42867, RR-00165, and U01 MH081896; and James S. McDonnell Foundation Grants 22002078, 220020165, and 220020293. A.M.M.S. is supported by a fellowship from the Portuguese Foundation for Science and Technology.

1. Leigh SR (2004) Brain growth, life history, and cognition in primate and human evolution. *Am J Primatol* 62:139–164.
2. Somel M, et al. (2009) Transcriptional neoteny in the human brain. *Proc Natl Acad Sci USA* 106:5743–5748.
3. Huttenlocher PR, Dabholkar AS (1997) Regional differences in synaptogenesis in human cerebral cortex. *J Comp Neurol* 387:167–178.
4. Petanjek Z, et al. (2011) Extraordinary neoteny of synaptic spines in the human prefrontal cortex. *Proc Natl Acad Sci USA* 108:13281–13286.
5. Gibson KR (1970) *Sequence of Myelinization in the Brain of Macaca mulatta* (University of California, Berkeley).
6. Yakovlev PI, Lecours A (1967) The myelogenetic cycles of regional maturation of the brain. *Regional Development of the Brain in Early Life*, ed Minkowski A (Blackwell Science, Oxford), pp 3–70.
7. Knickmeyer RC, et al. (2010) Maturational trajectories of cortical brain development through the pubertal transition: Unique species and sex differences in the monkey revealed through structural magnetic resonance imaging. *Cereb Cortex* 20: 1053–1063.
8. Sakai T, et al. (2011) Differential prefrontal white matter development in chimpanzees and humans. *Curr Biol* 21:1397–1402.
9. Sherwood CC, et al. (2011) Aging of the cerebral cortex differs between humans and chimpanzees. *Proc Natl Acad Sci USA* 108:13029–13034.
10. Simons M, Trajkovic K (2006) Neuron-glia communication in the control of oligodendrocyte function and myelin biogenesis. *J Cell Sci* 119:4381–4389.
11. Wake H, Lee PR, Fields RD (2011) Control of local protein synthesis and initial events in myelination by action potentials. *Science* 333:1647–1651.
12. Davis KL, et al. (2003) White matter changes in schizophrenia: Evidence for myelin-related dysfunction. *Arch Gen Psychiatry* 60:443–456.
13. Schlösser RG, et al. (2007) White matter abnormalities and brain activation in schizophrenia: A combined DTI and fMRI study. *Schizophr Res* 89:1–11.
14. Höistad M, et al. (2009) Linking white and grey matter in schizophrenia: Oligodendrocyte and neuron pathology in the prefrontal cortex. *Front Neuroanat* 3:9.
15. Dracheva S, et al. (2006) Myelin-associated mRNA and protein expression deficits in the anterior cingulate cortex and hippocampus in elderly schizophrenia patients. *Neurobiol Dis* 21:531–540.
16. Hakak Y, et al. (2001) Genome-wide expression analysis reveals dysregulation of myelination-related genes in chronic schizophrenia. *Proc Natl Acad Sci USA* 98: 4746–4751.
17. McCullumsmith RE, et al. (2007) Expression of transcripts for myelination-related genes in the anterior cingulate cortex in schizophrenia. *Schizophr Res* 90:15–27.
18. Mitkus SN, et al. (2008) Expression of oligodendrocyte-associated genes in dorsolateral prefrontal cortex of patients with schizophrenia. *Schizophr Res* 98:129–138.

19. Harris LW, et al. (2009) Gene expression in the prefrontal cortex during adolescence: Implications for the onset of schizophrenia. *BMC Med Genomics* 2:28.
20. Barley K, Dracheva S, Byne W (2009) Subcortical oligodendrocyte- and astrocyte-associated gene expression in subjects with schizophrenia, major depression and bipolar disorder. *Schizophr Res* 112:54–64.
21. Davis KL, Haroutunian V (2003) Global expression-profiling studies and oligodendrocyte dysfunction in schizophrenia and bipolar disorder. *Lancet* 362:758.
22. Hof PR, et al. (2003) Loss and altered spatial distribution of oligodendrocytes in the superior frontal gyrus in schizophrenia. *Biol Psychiatry* 53:1075–1085.
23. Edgar JM, et al. (2009) Early ultrastructural defects of axons and axon-glia junctions in mice lacking expression of Cnp1. *Glia* 57:1815–1824.
24. Quarles RH (2007) Myelin-associated glycoprotein (MAG): Past, present and beyond. *J Neurochem* 100:1431–1448.
25. Groeschel S, Vollmer B, King MD, Connelly A (2010) Developmental changes in cerebral grey and white matter volume from infancy to adulthood. *Int J Dev Neurosci* 28:481–489.
26. Gogtay N, et al. (2004) Dynamic mapping of human cortical development during childhood through early adulthood. *Proc Natl Acad Sci USA* 101:8174–8179.
27. Shaw P, et al. (2008) Neurodevelopmental trajectories of the human cerebral cortex. *J Neurosci* 28:3586–3594.
28. Sowell ER, Thompson PM, Holmes CJ, Jernigan TL, Toga AW (1999) In vivo evidence for post-adolescent brain maturation in frontal and striatal regions. *Nat Neurosci* 2: 859–861.
29. Herrmann E, Call J, Hernàndez-Lloreda MV, Hare B, Tomasello M (2007) Humans have evolved specialized skills of social cognition: The cultural intelligence hypothesis. *Science* 317:1360–1366.
30. Abrahám H, et al. (2010) Myelination in the human hippocampal formation from midgestation to adulthood. *Int J Dev Neurosci* 28:401–410.
31. Benes FM (1989) Myelination of cortical-hippocampal relays during late adolescence. *Schizophr Bull* 15:585–593.
32. Benes FM, Turtle M, Khan Y, Farol P (1994) Myelination of a key relay zone in the hippocampal formation occurs in the human brain during childhood, adolescence, and adulthood. *Arch Gen Psychiatry* 51:477–484.
33. Brody BA, Kinney HC, Kloman AS, Gilles FH (1987) Sequence of central nervous system myelination in human infancy. I. An autopsy study of myelination. *J Neuropathol Exp Neurol* 46:283–301.
34. Gilles FH (1976) Myelination in the neonatal brain. *Hum Pathol* 7:244–248.
35. Hildebrand C, Remahl S, Persson H, Bjartmar C (1993) Myelinated nerve fibres in the CNS. *Prog Neurobiol* 40:319–384.
36. Kinney HC, Brody BA, Kloman AS, Gilles FH (1988) Sequence of central nervous system myelination in human infancy. II. Patterns of myelination in autopsied infants. *J Neuropathol Exp Neurol* 47:217–234.
37. Preuss TM, Goldman-Rakic PS (1991) Myelo- and cytoarchitecture of the granular frontal cortex and surrounding regions in the strepsirhine primate *Galago* and the anthropoid primate *Macaca*. *J Comp Neurol* 310:429–474.
38. Robson SL, Wood BA (2008) Hominin life history: Reconstruction and evolution. *J Anat* 212:394–425.
39. Bartzokis G, et al. (2010) Lifespan trajectory of myelin integrity and maximum motor speed. *Neurobiol Aging* 31:1554–1562.
40. Elston GN, Oga T, Fujita I (2009) Spinogenesis and pruning scales across functional hierarchies. *J Neurosci* 29:3271–3275.
41. Huttenlocher PR (1979) Synaptic density in human frontal cortex - developmental changes and effects of aging. *Brain Res* 163:195–205.
42. Jacobs B, Driscoll L, Schall M (1997) Life-span dendritic and spine changes in areas 10 and 18 of human cortex: A quantitative Golgi study. *J Comp Neurol* 386:661–680.
43. Jacobs B, et al. (2001) Regional dendritic and spine variation in human cerebral cortex: A quantitative Golgi study. *Cereb Cortex* 11:558–571.
44. Travis K, Ford K, Jacobs B (2005) Regional dendritic variation in neonatal human cortex: A quantitative Golgi study. *Dev Neurosci* 27:277–287.
45. Gravel M, et al. (2009) 2′,3′-Cyclic nucleotide 3′-phosphodiesterase: A novel RNA-binding protein that inhibits protein synthesis. *J Neurosci Res* 87:1069–1079.
46. Lee PR, Fields RD (2009) Regulation of myelin genes implicated in psychiatric disorders by functional activity in axons. *Front Neuroanat* 3:4.
47. Li M, et al. (1996) Myelin-associated glycoprotein inhibits neurite/axon growth and causes growth cone collapse. *J Neurosci Res* 46:404–414.
48. Yin X, et al. (1998) Myelin-associated glycoprotein is a myelin signal that modulates the caliber of myelinated axons. *J Neurosci* 18:1953–1962.
49. Bogin B (1999) Evolutionary perspective on human growth. *Annu Rev Anthropol* 28: 109–153.
50. Blakemore SJ, Choudhury S (2006) Development of the adolescent brain: implications for executive function and social cognition. *J Child Psychol Psychiatry* 47:296–312.
51. Bartzokis G (2002) Schizophrenia: Breakdown in the well-regulated lifelong process of brain development and maturation. *Neuropsychopharmacology* 27:672–683.
52. Fields RD (2008) White matter in learning, cognition and psychiatric disorders. *Trends Neurosci* 31:361–370.
53. Leigh SR, Park PB (1998) Evolution of human growth prolongation. *Am J Phys Anthropol* 107:331–350.
54. Kang HJ, et al. (2011) Spatio-temporal transcriptome of the human brain. *Nature* 478: 483–489.
55. Pistorio AL, Hendry SH, Wang X (2006) A modified technique for high-resolution staining of myelin. *J Neurosci Methods* 153:135–146.
56. Mouton PR, Gokhale AM, Ward NL, West MJ (2002) Stereological length estimation using spherical probes. *J Microsc* 206:54–64.
57. Sherwood CC, et al. (2010) Neocortical synaptophysin asymmetry and behavioral lateralization in chimpanzees (*Pan troglodytes*). *Eur J Neurosci* 31:1456–1464.
58. Zar JH (2010) *Biostatistical Analysis* (Prentice Hall, Upper Saddle River, NJ), 5th Ed.
59. Kennedy GE (2005) From the ape's dilemma to the weanling's dilemma: Early weaning and its evolutionary context. *J Hum Evol* 48:123–145.
60. Littleton J (2005) Fifty years of chimpanzee demography at Taronga Park Zoo. *Am J Primatol* 67:281–298.

Supporting Information

Miller et al. 10.1073/pnas.1117943109

SI Materials and Methods

Sample. ***Humans.*** Human brain specimens from the Yakovlev–Haleem collection were fixed in 10% (vol/vol) formalin, prepared in whole-brain serial celloidin sections, cut at a uniform thickness of 35 μm, and stained using the Loyez technique for myelinated fibers (1). Tissue from the National Institute of Child Health and Human Development Brain and Tissue Bank was fixed in 10% buffered formalin, cut at a uniform thickness of 40 μm, and stained using a modified Gallyas technique for myelinated fibers (2). Tissue from the laboratory of Nenad Šestan at Yale University (New Haven, CT) was snap-frozen in isopentane and stored at −80 °C (detailed in ref. 3).

Chimpanzees. The chimpanzee brain specimens were collected postmortem from various research institutions and fixed by immersion in 10% buffered formalin for variable lengths of time, transferred to a PBS solution containing 0.1% sodium azide, and stored at 4 °C. Blocks of ∼3 cm were sectioned perpendicular to the pial surface containing a single gyrus from the regions of interest in the left hemisphere (right hemisphere was used in a single case; Table S1). Tissue blocks were cryoprotected by immersion in buffered sucrose solutions up to 30%, embedded in tissue medium, frozen in a slurry of dry ice and isopentane, and sectioned at 40 μm. Every 10th section (400 μm apart) was stained for Nissl substance with a solution of 0.5% cresyl violet to visualize cytoarchitecture. An adjacent 1-in-10 series of sections was stained using a modified Gallyas silver impregnation method to reveal myelinated axons (2) (Table S1).

Human brain specimens ($n = 24$) in the Yakovlev–Haleem slide collection were prepared using the Loyez method, as were control chimpanzee specimens ($n = 5$). The Loyez protocol follows incubation in hematoxylin and alcohol with a developer consisting of potassium ferricyanide, sodium borate, and water, with a rinsing step with ammonium hydroxide, to visualize myelinated fibers (1). Chimpanzee brain sections ($n = 20$) were prepared by using a modified Gallyas silver impregnation protocol, as were control human sections ($n = 9$). The Gallyas protocol follows incubation in pyridine and acetic anhydride with a developer consisting of formalin, ammoniacal silver nitrate, and paraformaldehyde, a silver granule cleansing step with low concentrations of acetic acid, and a bleaching step using potassium ferricyanide, to visualize myelinated fibers. An adjacent 1-in-10 series of sections in all samples were stained for Nissl.

Stereology. Myelinated fiber length density (MFLD) in both samples was quantified by the same observer (D.J.M.) using a computerized stereology system consisting of a Zeiss Axioplan 2 (for chimpanzees) or Nikon E1000M (for humans) microscope and StereoInvestigator software (MBF Bioscience). By using adjacent Nissl-stained sections, we confirmed the cytoarchitecture of regions of interest and located the white matter–gray matter interface. Beginning at a random starting point, three myelin-stained sections equidistantly spaced within 1,200 μm (chimpanzees) or 1,050 μm (humans) were selected for analysis. MFLD was evaluated using the SpaceBalls probe, a 6-μm sampling hemisphere for lineal features combined with a fractionator sampling scheme (4). Fibers were marked where they intersected the outline of the hemispheric probe. Sampling hemispheres were placed in a systematic random fashion every 700 × 700 μm to cover the region of interest with ∼30 frames per section, and mean mounted section thickness was measured at every 10 sampling locations. The analysis was performed under Koehler illumination at 60× (humans), 63× (chimpanzees), or 100× (control samples). To obtain MFLD, the total fiber length was divided by the planimetric measurement of the reference volume that was sampled, as calculated by the StereoInvestigator software.

Western Blot Analysis. Protein expression analysis of tissue sections adjacent to those used for stereology was performed in chimpanzees by Western blot assay. Frozen tissue samples from human were used for Western blotting. Tissue (50–100 mg) was homogenized in radioimmunoprecipitation assay buffer (pH 7.6) containing 2% SDS and protease inhibitors, and the contents were incubated at 100 °C for 20 min followed by incubation at 60 °C for 2 h. The tissue lysates were then centrifuged at 15,000 × *g* for 20 min at 4 °C. Protein concentrations were measured with the DC protein assay (Bio-Rad) after detergent solubilization. Protein samples were diluted 1:1 in Laemmli sample buffer and boiled for 10 min. Samples were separated on NuPAGE Novex 4% to 12% Bis-Tris gel (Invitrogen). The proteins were electrotransferred to a PVDF membrane in Tris-glycine-methanol buffer. The membrane was blocked for 1 h at room temperature in a blocking solution mixture with 5% nonfat dry milk in 0.05% Tween 20 and Tris-buffered saline solution (pH 8.0). The membrane was washed with Tris-buffered saline solution with Tween 20 on a shaker at room temperature three times for 10 min and incubated overnight at 4 °C with the following antibodies: rabbit anti–myelin-associated glycoprotein (MAG; 1:300; LifeSpan BioSciences), mouse anti–2′,3′-cyclic nucleotide 3′-phosphodiesterase (CNP; 1:300; Abcam), anti–β-actin polyclonal antibody (1:1,000; Santa Cruz Biotechnology), and anti-GAPDH polyclonal antibody (1:500; Imgenex) in 1% nonfat dry milk in Tris-buffered saline solution with Tween 20. After repeated washing, the membrane was incubated with horseradish peroxidase-conjugated goat anti-mouse IgG or donkey anti-rabbit IgG (1:3,000; Santa Cruz Biotechnology) overnight at 4 °C. After washing, immunoreactivity was visualized by using a chemiluminescent substrate (ECL; Amersham Biosciences; Figs. S2 and S3*C*). Densitometry analyses were performed to quantify signals generated by Western blotting with Scion Image software. In chimpanzees, the immunodetected bands were then normalized to total protein in each sample. To account for blot-to-blot variation in exposure and film development, three concentrations of a blotting standard were loaded onto each gel. The standard comprised a mixture of protein samples from the four cerebral cortex regions of each individual chimpanzee used in the study. The intensity of the bands for each unknown sample was normalized to this standard. In human samples, densitometric measurements were normalized to an anti–β-actin loading control.

1. Yakovlev PI, Lecours A (1967) The myelogenetic cycles of regional maturation of the brain. *Regional Development of the Brain in Early Life*, ed Minkowski A (Blackwell Science, Oxford), pp 3–70.
2. Pistorio AL, Hendry SH, Wang X (2006) A modified technique for high-resolution staining of myelin. *J Neurosci Methods* 153:135–146.
3. Kang HJ, et al. (2011) Spatio-temporal transcriptome of the human brain. *Nature* 478: 483–489.
4. Mouton PR, Gokhale AM, Ward NL, West MJ (2002) Stereological length estimation using spherical probes. *J Microsc* 206:54–64.

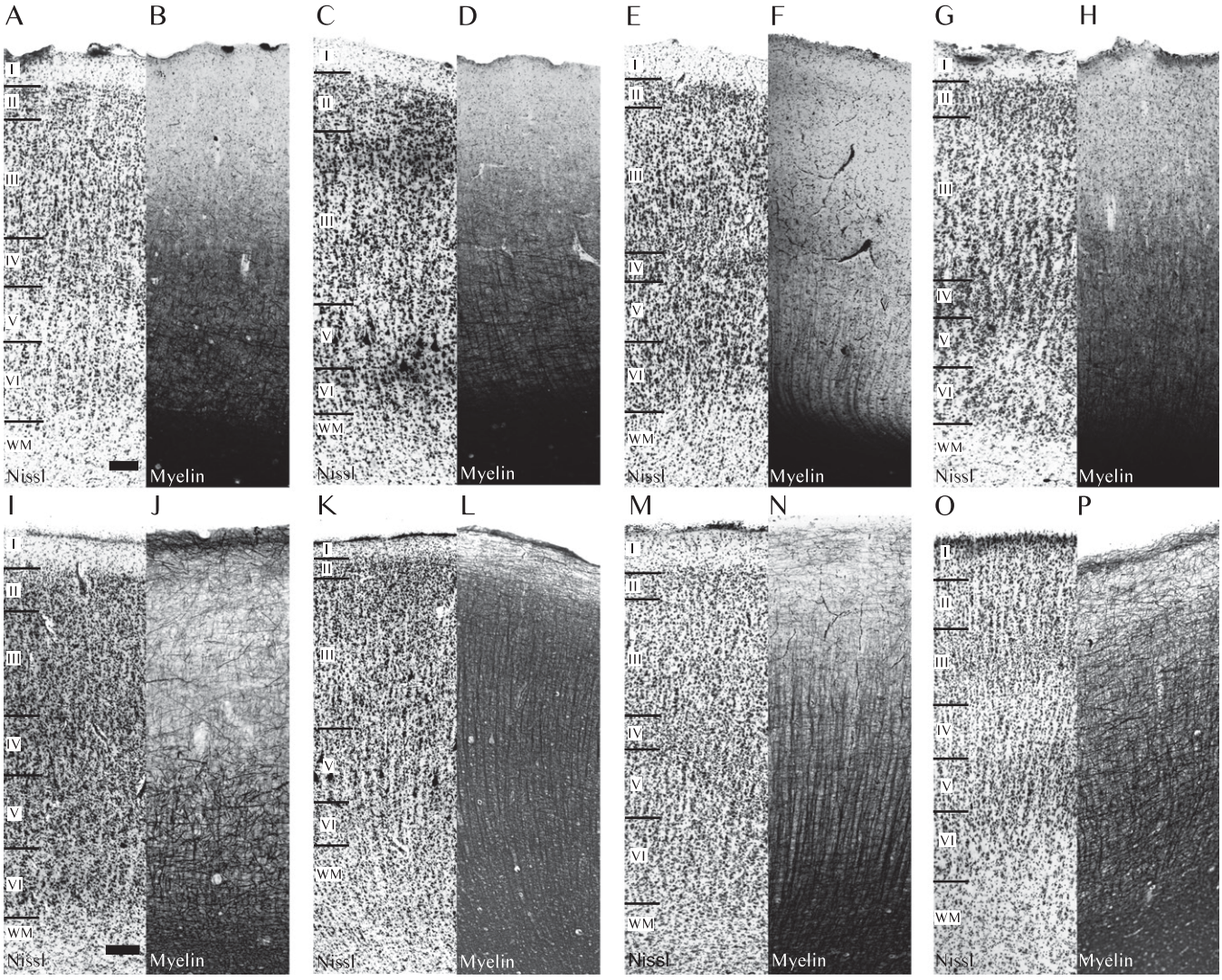

Fig. S1. Neocortical regions of interest in adult humans and chimpanzees. Representative sections from each region of interest (somatosensory, *A, B, I,* and *J*; motor, *C, D, K*, and *L*; frontopolar, *E, F, M,* and *N*; and visual, *G, H, O, P*) stained for cytoarchitecture (Nissl) and myelinated axons (myelin) in adjacent sections in adult humans (*A–F*) and chimpanzees (*G–L*). Nissl-stained sections are subdivided into layers I to VI. White matter (WM) is demarcated at the bottom of the cortex. (Scale bar: 200 μm.)

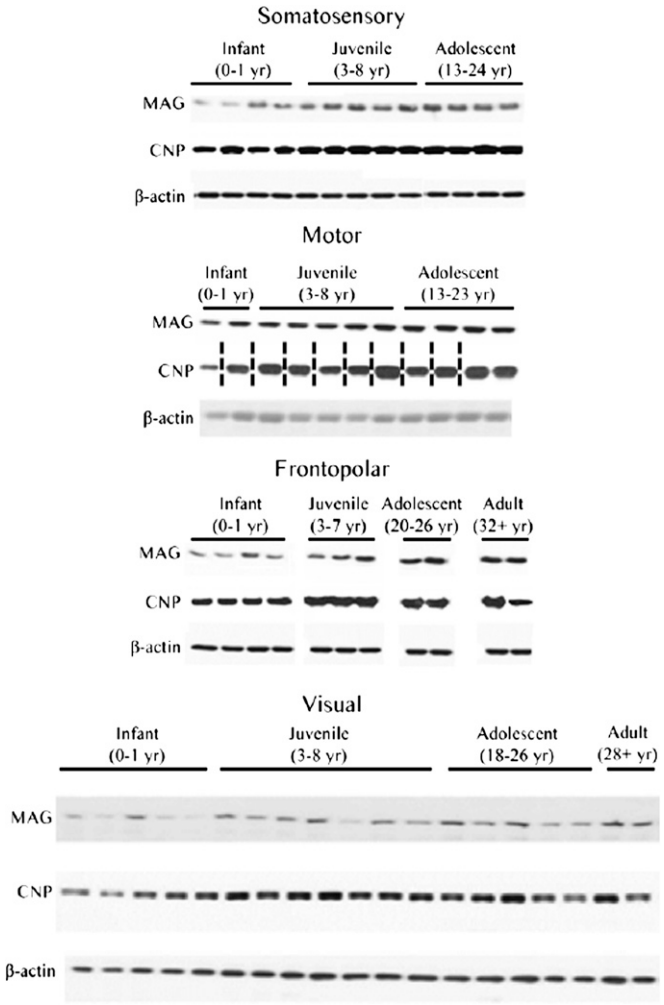

Fig. S2. Immunoblots depicting MAG and CNP protein expression in humans. Representative Western blots of MAG and CNP extracted from frozen human neocortex, arranged by age in years (0–1 y, infant; 3–8 y, juvenile; 13–26 y, adolescent/young adult; and ≥28 y, adult) and region of interest (somatosensory, areas 3a, 3b, 1, and 2; motor, area 4; frontopolar, area 10; and visual, areas 17/V1 and 18/V2). Vertical bars on the blot specify where only one band per sample was used for the representative figure. In the original blot, samples were run in duplicate. Adjustments of brightness were applied to whole images of gels immunoblotted with anti-CNP and anti–β-actin antibodies to facilitate densitometry analysis.

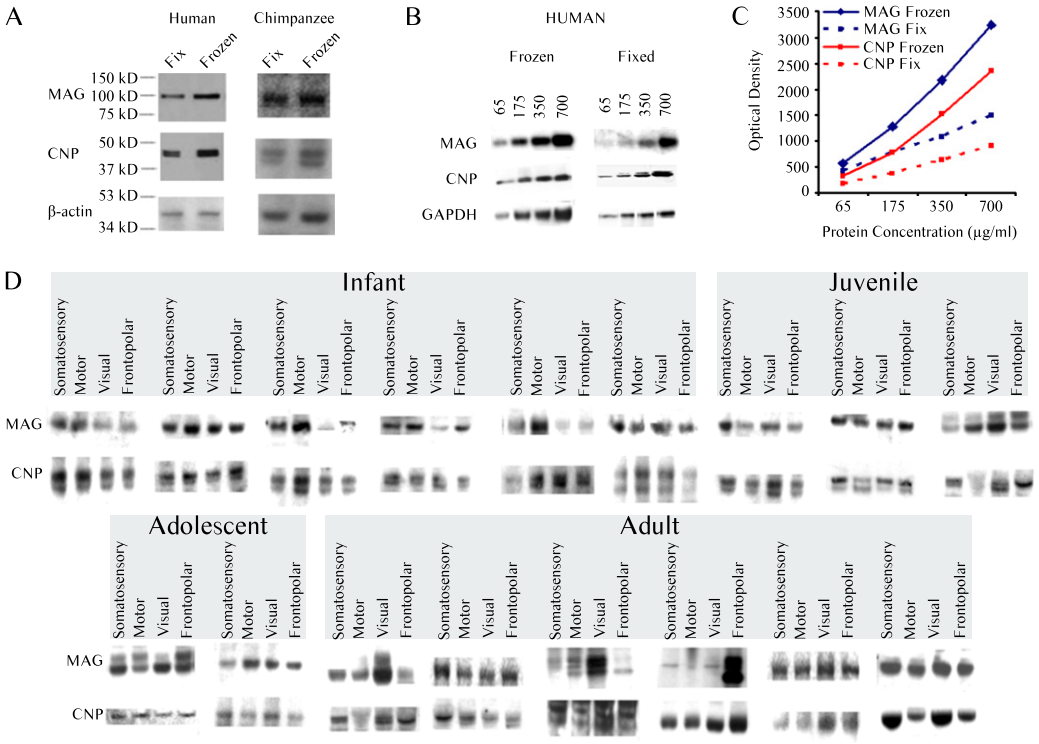

Fig. S3. MAG and CNP protein expression profile in chimpanzee neocortical regions: Western blot analysis validation and representative immunoblots. (*A*) SDS/PAGE pattern of MAG and CNP extracted from formalin-fixed tissue is comparable to that extracted from fresh frozen tissue, as compared between and within species. (*B*) Representative immunoblot of MAG and CNP protein expression analysis in frozen and formalin-fixed tissue producing a linear relationship between protein concentrations. (*C*) Plot of optical density standard curve in Western blot assays used to determine that tissue samples fell within the linear portion of the densitometric curve. (*D*) Representative Western blots of MAG and CNP, arranged by age (0–2 y, infant; 5–6 y, juvenile; 9–11 y, adolescent; and ≥17 y, adult) in years and region of interest (somatosensory, area 3b/3a/1/2; motor, area 4; frontopolar, area 10; and visual, areas 17/V1 and 18/V2).

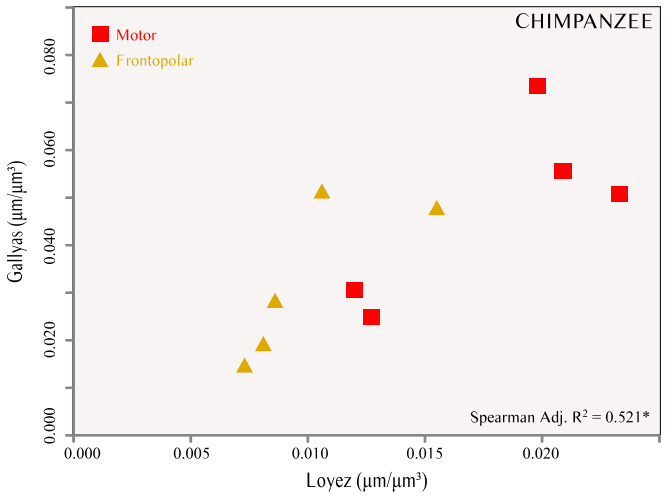

Fig. S4. Interprotocol correlation in chimpanzees. Correlation between the same chimpanzee specimens stained using the Gallyas (*y*-axis) (1) and Loyez (*x*-axis) (2) protocols (n = 5 per region of interest; units are μm/μm^3). Squares represent motor cortex area (area 4) and triangles represent frontopolar cortex (area 10). Nonparametric Spearman adjusted R^2 is reported (*P < 0.05).

1. Pistorio AL, Hendry SH, Wang X (2006) A modified technique for high-resolution staining of myelin. *J Neurosci Methods* 153:135–146.
2. Yakovlev PI, Lecours A (1967) The myelogenetic cycles of regional maturation of the brain. *Regional Development of the Brain in Early Life*, ed Minkowski A (Blackwell Science, Oxford), pp 3–70.

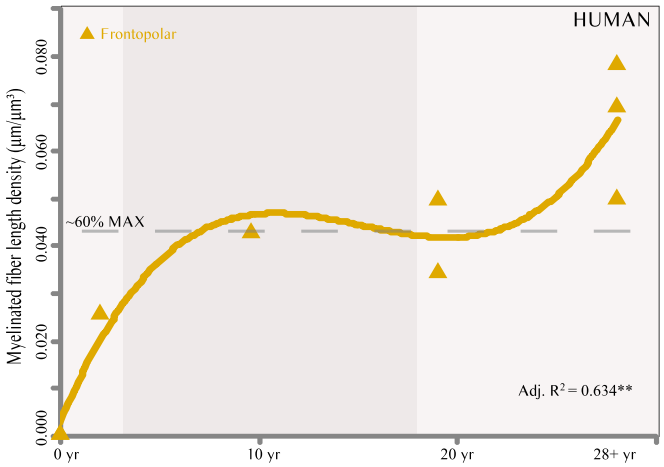

Fig. S5. Developmental trajectory of MFLD in human controls. Best-fit curves for data in human control sections stained by using the Gallyas protocol for myelin by age in years (0–1 y, infant; 3–8 y, juvenile; 13–26 y, adolescent/young adult; ≥28 y, adult). The shaded vertical area represents time between weaning and full sexual maturation. Triangles represent frontopolar cortex (area 10). Dashed line represents 60% of maximum adult MFLD in the sample (**$P < 0.01$; $n = 9$).

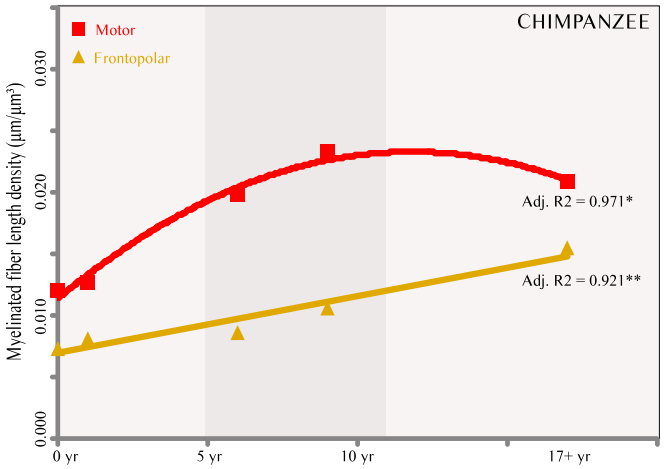

Fig. S6. Developmental trajectory of MFLD in chimpanzee controls. Best-fit curves for data in chimpanzee control sections stained using the Loyez protocol for myelin (1) (*SI Materials and Methods*) by age in years. The shaded vertical area represents time between weaning and full sexual maturation. Squares represent motor cortex (area 4) and triangles represent frontopolar cortex (area 10). (*$P < 0.05$ and **$P < 0.01$; $n = 5$ per region of interest).

1. Yakovlev PI, Lecours A (1967) The myelogenetic cycles of regional maturation of the brain. *Regional Development of the Brain in Early Life*, ed Minkowski A (Blackwell Science, Oxford), pp 3–70.

Table S1. Specimens used in this study

Species	Age	Sex	Hemisphere	Stain
Human	Stillborn	M	Left	Loyez
Human	Stillborn	F	Left	Loyez
Human	Stillborn	F	Left	Loyez
Human	Stillborn	F	Left	Loyez
Human	Stillborn	F	Left	Loyez
Human	Stillborn	F	Left	Gallyas
Human	Stillborn	M	Left	Gallyas
Human	6 wk	F	Left	Loyez
Human	4 mo	M	Left	Western blot
Human	7 mo	M	Left	Loyez
Human	9 mo	M	Left	Loyez
Human	10 mo	M	Left	Western blot
Human	1 y	F	Left	Western blot
Human	2.8 y	Unknown	Left	Gallyas
Human	3 y	M	Left	Western blot
Human	3 y	F	Left	Western blot
Human	3.5 y	M	Left	Loyez
Human	4 y	F	Left	Loyez
Human	4 y	F	Left	Loyez
Human	5 y	M	Left	Loyez
Human	6 y	M	Left	Loyez
Human	6.5 y	M	Left	Loyez
Human	8 y	M	Left	Western blot
Human	9.5 y	F	Left	Loyez
Human	9.6 y	F	Left	Gallyas
Human	11 y	F	Left	Loyez
Human	13 y	F	Left	Western blot
Human	16 y	F	Left	Loyez
Human	18 y	M	Left	Western blot
Human	19 y	M	Left	Gallyas
Human	19 y	M	Left	Gallyas
Human	20 y	M	Left	Loyez
Human	22 y	M	Left	Western blot
Human	23 y	F	Left	Loyez
Human	23 y	M	Left	Western blot
Human	25 y	Unknown	Left	Western blot
Human	26 y	Unknown	Left	Western blot
Human	28 y	M	Left	Loyez
Human	28.5 y	M	Left	Gallyas
Human	32 y	F	Left	Loyez
Human	32 y	Unknown	Left	Western blot
Human	41 y	F	Left	Gallyas
Human	44 y	M	Left	Gallyas
Human	44 y	M	Left	Loyez
Human	47 y	F	Left	Loyez
Human	47 y	Unknown	Left	Western blot
Human	50 y	M	Left	Loyez
Chimpanzee	Stillborn	F	Left	Gallyas
Chimpanzee	Stillborn	F	Left	Gallyas/Western blot
Chimpanzee	Stillborn	M	Left	Gallyas
Chimpanzee	Stillborn	M	Left	Gallyas
Chimpanzee	1 wk	M	Left	Gallyas/Western blot
Chimpanzee	2 wk	M	Left	Gallyas/Western blot
Chimpanzee	1 y	Unknown	Left	Western blot
Chimpanzee	1 y	M	Left	Gallyas/Loyez
Chimpanzee	1.5 y	Unknown	Left	Gallyas/Western blot
Chimpanzee	2 y	F	Left	Gallyas/Western blot
Chimpanzee	5 y	M	Left	Gallyas/Western blot
Chimpanzee	5.3 y	M	Right	Gallyas/Western blot
Chimpanzee	6 y	M	Left	Gallyas/Loyez/Western
Chimpanzee	9 y	M	Left	Gallyas/Loyez/Western
Chimpanzee	11 y	M	Left	Gallyas/Loyez/Western
Chimpanzee	17 y	M	Left	Gallyas/Western blot

Table S1. Cont.

Species	Age	Sex	Hemisphere	Stain
Chimpanzee	19 y	M	Left	Gallyas/Western blot
Chimpanzee	19 y	F	Left	Gallyas/Western blot
Chimpanzee	27 y	M	Left	Gallyas/Western blot
Chimpanzee	35 y	F	Left	Gallyas/Western blot
Chimpanzee	41 y	F	Left	Gallyas/Loyez/Western

Table S2. Percent of maximal, mature adult MFLD during different developmental stages (mean ± SEM)

	Human			Chimpanzee		
Category	Infant (0–1 y)	Juvenile (3–9 y)	Adolescent/ young adult (11–23 y)	Infant (0-2 y)	Juvenile (5–7 y)	Adolescent/ young adult (9–11 y)
No. of individuals	8	7	4	9	3	2
Somatosensory	2.4 ± 2.1	45.1 ± 4.3	65.7 ± 7.2	14.6 ± 6.6	58.4 ± 14.2	97.3 ± 23.8
Motor	3.7 ± 2.2	61.3 ± 2.3	71.4 ± 13.8	18.2 ± 7.8	82.3 ± 25.5	106.3 ± 18.1
Frontopolar	0.1 ± 0.1	28.3 ± 1.9	61.5 ± 7.8	16.2 ± 7.9	57.1 ± 17.1	93.4 ± 49.0
Visual	0.3 ± 0.2	33.0 ± 1.6	61.4 ± 5.6	17.9 ± 8.8	74.7 ± 23.1	86.9 ± 25.2
Control frontopolar	1.5*	52.5*	64.2*	49.7*	55.5†	68.4†
Control motor	—	—	—	59.1*	94.7†	111.4†

*n = 2.
†n = 1.

Table S3. Best-fit regression functions for protein expression data

Function	Function	Adjusted R^2	P value
Humans			
CNP			
Somatosensory	Linear	0.149	0.029*
Motor	Linear	−0.007	0.387
Frontopolar	Quadratic	0.425	0.046*
Visual	Cubic	0.273	0.051*
MAG			
Somatosensory	Linear	0.174	0.02*
Motor	Linear	−0.021	0.559
Frontopolar	Quadratic	0.530	0.038*
Visual	Linear	0.169	0.006†
Chimpanzees			
CNP			
Somatosensory	Linear	0.155	0.043*
Motor	Quadratic	0.106	0.074
Frontopolar	Linear	0.113	0.110
Visual	Quadratic	0.053	0.118
MAG			
Somatosensory	Quadratic	0.158	0.129
Motor	Quadratic	0.159	0.052*
Frontopolar	Linear	0.541	0.001*
Visual	Linear	0.173	0.061

Values calculated by using hierarchical multiple regression analysis with adults as endpoint (*Materials and Methods*). Parametric Spearman adjusted R^2 values are reported. Significant at *$P < 0.05$ or †$P < 0.01$.